ACS Catalysis

Research Article

pubs.acs.org/acscatalysis

Comparative Theoretical Study of the Ring-Opening Polymerization of Caprolactam vs Caprolactone Using QM/MM Methods

Brigitta Elsässer,* Iris Schoenen, and Gregor Fels

Department of Chemistry, University of Paderborn, Warburger Strasse 100, D-33098 Paderborn, Germany

Supporting Information

ABSTRACT: *Candida antarctica lipase B* (CALB) efficiently catalyzes the ring-opening polymerization of lactones to high molecular weight products in good yield. In contrast, an efficient enzymatic synthesis of polyamides has so far not been described in the literature. This obvious difference in enzyme catalysis is the subject of our comparative study of the initial steps of a CALB catalyzed ring-opening polymerization of ε-caprolactone and ε-caprolactam. We have applied docking tools to generate the reactant state complex and performed quantum mechanical/molecular mechanical (QM/MM) calculations at the density functional theory (DFT) PBE0 level of theory to simulate the acylation of Ser105 by the lactone and the lactam, respectively, via the corresponding first tetrahedral intermediates. We could identify a decisive difference in the accessibility of the two substrates in the ring-opening to the respective acyl enzyme complex as the attack of ε-caprolactam is hindered because of an energetically disfavored proton transfer during this part of the catalytic reaction while ε-caprolactone is perfectly processed along the widely accepted pathway using the catalytic triade of Ser105, His224, and Asp187. Since the generation of an acylated Ser105 species is the crucial step of the polymerization procedure, our results give an explanation for the unsatisfactory enzymatic polyamide formation and opens up new possibilities for targeted rational catalyst redesign in hope of an experimentally useful CALB catalyzed polyamide synthesis

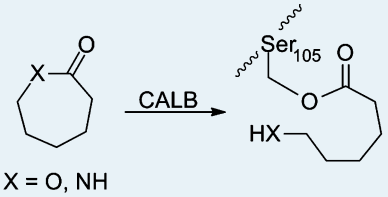

KEYWORDS: *ring-opening polymerization, CALB, ε-caprolactam, ε-caprolactone, DFT, QM/MM, NEB*

INTRODUCTION

Polyamides are industrially synthesized by ring-opening polymerization of lactams or by condensation reaction between diamines and diacids. Both reactions only proceed under relatively harsh conditions of high temperature and pressure, catalyzed by strong acids or metal-containing catalysts.[1,2] As an alternative, enzyme catalyzed polymerization has been recognized as a powerful bioinspired procedure that facilitates reactions under mild conditions by sustainable chemical processes, which even are accepted for preparation of biomedical material.[3−5] In this respect, polyesters are readily available through enzymatic catalysis by ring-opening polymerization of lactones as well as from condensation of ω-hydroxyesters, or diols with diesters, respectively.[6−11] In contrast, only very few enzymatic syntheses of polyamides can be found in the literature.[12−16]

Cheng[13] as well as Gu[15] and co-workers, for instance, describe the polycondensation of diacids like adipic, malonic, and fumaric acid with diethylene triamine and triethylene tetramine. It is, however, remarkable that simple diamines like 1,6-hexamethylene diamine have not been employed in these reactions despite the fact that the analogue 1,6-dihydroxyhexane has successfully been used to build polyesters by condensation with diacids.[17] So far, the first and only published enzyme catalyzed polyamide synthesis from lactams is the *candida antarctica* lipase B (CALB) catalyzed polymerization of β-lactam (2-azetidinon) to unbranched poly(β-alanine) published by Schwab et al.[14,16] But even this approach only resulted in an oligomeric material with a maximum chain length of 18 monomer units and an average length of 8 units. In this respect it should be noted that various other enzyme catalyzed ring-opening reactions of substituted β-lactams are reported in the literature, none of which, however, is a polymerization reaction.[18−21]

Uyama et al.[22] have postulated a mechanism of the ring-opening polymerization of lactones, and it was suggested that this mechanism also applies for the ring-opening polymerization of lactams (path B in Scheme 1).[14] According to this mechanism, an acyl-enzyme intermediate is formed between the lactam and residue Ser105 of CALB which is hydrolyzed to the ω-amino acid by residual water present in the enzyme and later on used to elongate the polymer chain at the acylated enzyme.

Path B of this mechanism requires production of the amino acid in reserve which is stored in between inside the enzyme or in the solvent, respectively. However, path B seems rather unlikely, as in case of the CALB-catalyzed β-lactam polymerization it was shown that the ring opened β-alanine is not a substrate.[14,16] On the basis of these results, we have computationally simulated the underlying catalytic cycle, and we have proposed an alternative mechanism following path A,[12] which is in agreement with all experimental findings, including the pK_a dependent deactivation of CALB by organic acids.[23] Essential in this mechanism are not only the amino acids

Received: December 19, 2012
Revised: May 5, 2013
Published: May 13, 2013

   dx.doi.org/10.1021/cs3008297 | ACS Catal. 2013, 3, 1397−1405

Scheme 1. Mechanistic Routes of CALB-Catalyzed Ring-Opening Polymerization of Lactams

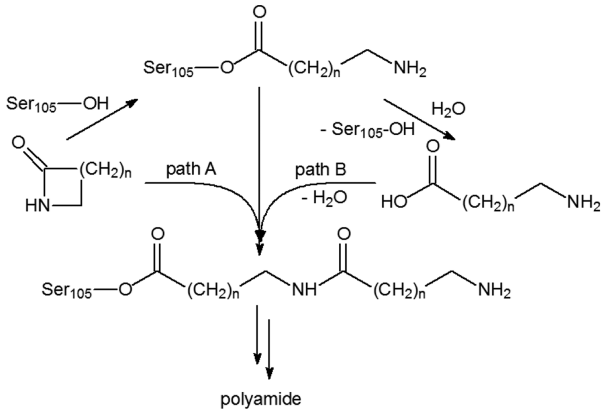

Ser105 and His224 but also the amino acids Thr40 and Gly106 which provide the stabilizing oxyanion hole but more importantly are also actively involved, both in handling a catalytic water molecule necessary for the ring-opening of the lactam as well as for chain elongation. According to this mechanism, β-lactam is initiating the polymerization by acylation of Ser105 and is successively in situ ring opened inside the active site pocket to β-alanine which itself elongates the polymer chain by inserting one after another into the acyl side chain of Ser105. In this way, the polymer chain is continuously growing out of the enzyme until it is liberated from the enzyme when a water molecule rather than a β-alanine unit reacts with the acyl-enzyme complex. This water molecule has to be contributed from the water reservoir of the immobilized enzyme. In general, this is not a limitation of the reaction because, for example, CALB catalyzed polymerizations of lactones are well-known from the literature so that obviously enough water is available even with dried enzyme preparations.[24−26]

The considerable differences of this proposed mechanism (path A) compared with the commonly assumed enzymatic polymerization mechanism (path B) prompted us to look into a direct comparison of a lactone and lactam polymerization, respectively, by computational chemistry methods, to possibly find a reason for the hitherto not understood differing reactivity of CALB with lactams and lactones. We have employed docking and quantum mechanical/molecular mechanical (QM/MM) calculations at the density functional theory (DFT) PBE0 level of theory in particular with ε-caprolactam and ε-caprolactone, respectively, to investigate at the atomistic level the details of the acylation of Ser105 by these two substrates as the initial step of the polymerization mechanism. Previous computational results of several groups[27−29] revealed that hydrogen bonding plays a crucial role in the enzyme catalysis especially the H-bond between the active site Serine and Glycine, as well as between Histidine and Aspartate. Therefore we also included these residues (Ser105, Gly107, His224, Asp134) among others, as described in the methods section.

Our results reveal a mechanistic difference in the CALB catalyzed polymerization of ε-caprolactone and ε-caprolactam and suggest that polyamide formation is inhibited by an energetically disfavorable proton transfer during the acylation step.

RESULTS AND DISCUSSION

Ring-Opening of ε-Caprolactone by Ser105. Experimental studies show that ε-caprolactone can be enzymatically polymerized by CALB with high molecular weight and excellent yield.[24−26] To generate a starting complex for our studies ε-caprolactone was first positioned at the alcohol side of the CALB active site by using the docking software QXP.[30] During the attack of Ser105 at the lactone carbonyl, two enantiomeric binding modes are possible resulting from the attack at the *Re*- or *Si*-side of the carbonyl group. Veld et al.[31] have studied the reactivity of various open chain *cisoid* and *transoid* lactones and they also distinguished between productive (*transoid*) and unproductive (*cisoid*) binding of the substrate depending on the nature of the ester bond. The structures of his first tetrahedral intermediates have (*R*)-configuration in case of productive binding mode and (*S*) for the unproductive one.

Our calculation starts with a docking procedure (*mcdock*) between ε-caprolactone and CALB resulting in almost equal proportions of the pseudo enantiomeric orientations which can be described as pre-*R*- and pre-*S*-configurations. Rescoring of the hits by the procedure described by Alisaraie et al.[32] yielded 3 productive binding modes according to the definition by Veld et al.[31] These structures were then used in consecutive docking runs (with restricted degrees of freedom for the lactone bonds, *mcldock*) to finally give a set of productive starting structures.

The best hit from this initial placement was optimized by the QM/MM method as described in the Methods section. Accordingly, in the reactant state (A) the monomer was stabilized by strong hydrogen bonds to (OH)Thr40 (2.68 Å, 149.9°). At this stage the HD(Ser105) proton points toward NE2(His224) (2.65 Å, 157.1°) and is in the correct geometry for a proton transfer. The substrate carbonyl is 3.37 Å away from OD(Ser105) and stays ready for a nucleophilic attack (reactant (**A**) in Scheme 2 and Figure 1, left).

The simulation of the nucleophilic attack of Ser105 on the substrate carbonyl was performed by the "spring method" as implemented in the NWChem.[33] Thus, a constraint of 1.6 Å was imposed between OD(Ser105) and the lactone carbonyl to generate a new single C−O bond. During the optimization process the HD(Ser105) proton was automatically transferred to NE2(His224) and a stable tetrahedral intermediate (B) was formed (Figure 1, right, Scheme 2). In the resulting intermediate (**B**, see Scheme 2) the ring oxygen of ε-

Scheme 2. Acylation of Ser105 by Caprolactone

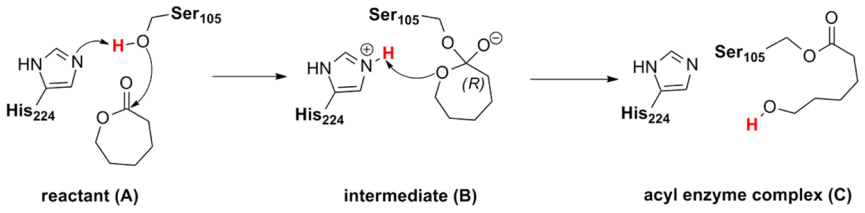

dx.doi.org/10.1021/cs3008297 | ACS Catal. 2013, 3, 1397−1405

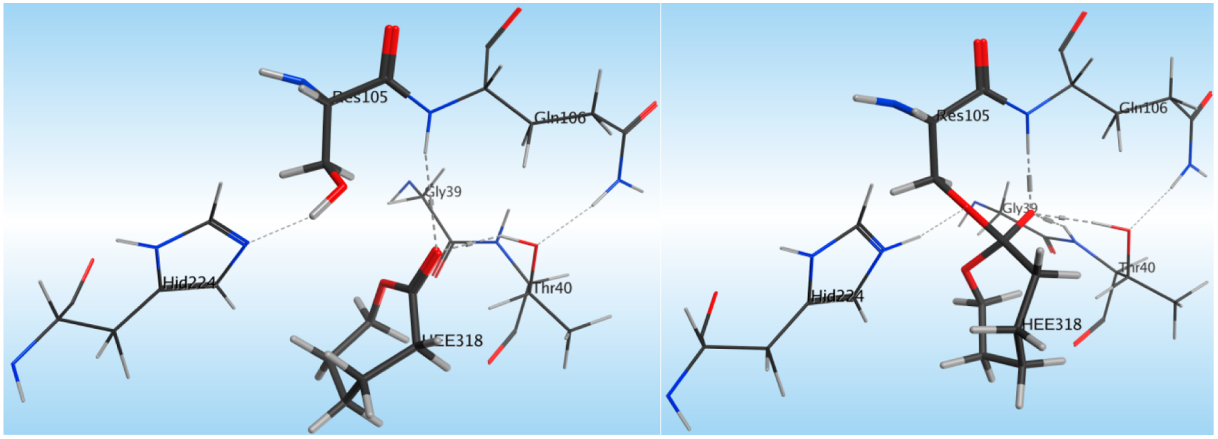

Figure 1. Reactant (**A**) (left) and intermediate (**B**) structure (right) of Scheme 2.

caprolactone is still positioned in front of His224 on the alcohol side of catalytic pocket and the former carbonyl carbon has *(R)*-configuration. The negatively charged oxygen is stabilized by three hydrogen bonds in the oxyanion hole (O(lactone)−NH(Gln106) is 2.73 Å, O(lactone)−OH(Thr40) are 2.66 Å and 3.11 Å, respectively) and by the positively charged NE2(His224).

In the next step of the reaction the lactone ring is opened by transferring the HE2(His224) proton to the lactone ring oxygen. Using a spring of 0.97 Å between these two atoms a QM/MM optimization resulted in the open-chain acyl enzyme complex (**C**) (Figure 2) in which the acyl-chain is positioned

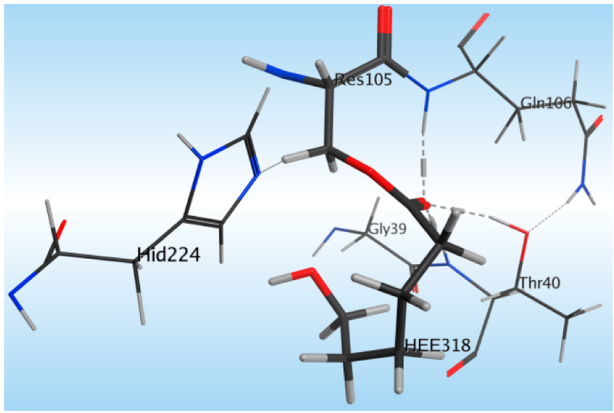

Figure 2. Ring-opened acyl enzyme complex (**C**) of Scheme 2.

on the acyl side of the pocket. With the help of docking techniques and QM/MM reoptimization the chain was unfolded resulting in reorientation toward the alcohol side of the active site. In both structures the carbonyl group is stabilized by the oxyanion hole, whereas in the unfolded docking structure the carbonyl is stabilized by Gln106 (O(carbonyl−NH(Gln106) is 2.81 Å) and Thr40 through two additional strong hydrogen bonds (O(carbonyl)−OH-(Thr40) is 2.68 Å and O(carbonyl)−NH(Thr40) is 3.04 Å).

Ring-Opening of ε-Caprolactam by Ser105. The reactant state complex with the lactam substrate (**D**, Scheme 3) was prepared similar to the procedure described for *ε*-caprolactone using docking and QM/MM optimization. Again we found a productive pre-R- and an unproductive pre-S-orientation with respect to the position of the nitrogen atom in the lactam ring. In the pre-S-orientation the nitrogen is oriented so that in the consecutive step (B→C) a proton shuttle from His224 would not be possible even not via water bridges. In contrast, in the pre-R-orientation the carbonyl is H-bonded to N(Gln106) 3.0 Å, OG(Ser105) 3.1 Å, and N(Thr40) 2.9 Å. The nitrogen has a strong H-bridge to Wat322, 2.8 Å.

To verify the difference of the two orientation in terms of productivity we processed both structures to simulate the nucleophilic attack of Ser105 on the carbonyl applying a spring of 1.6 Å between OG(Ser105) and the carbonyl oxygen. In case of the pre-S-orientation all of our attempts to generate the acyl-enzyme complex have failed. Even if we first tried to transfer the HG(Ser105) proton to His224 the remaining negatively charged Ser-oxygen did not attack the carbonyl. In contrast, in case of the pre-R-orientation the hydrogen transfer and attack proceeds successfully (from Wat322), and we have continued our calculations, therefore, with the pre-R-orientation only.

After removal of the spring the structure has been optimized and in the resulting complex we observed an unexpected

Scheme 3. Acylation of Ser105 by Caprolactam: Generation of the First Tetrahedral Intermediate (E) and Ring-Opening to the Acyl-Enzyme Complex (F)

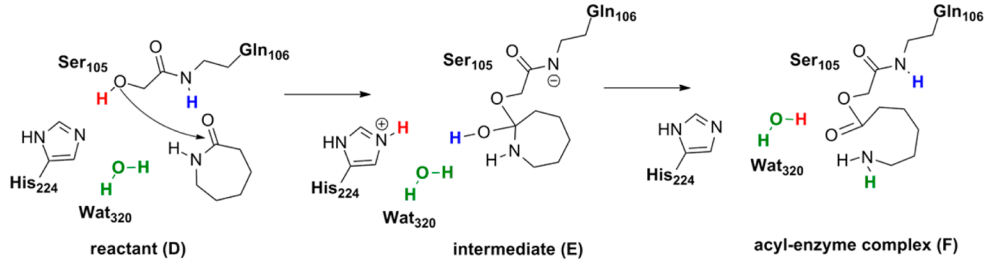

dx.doi.org/10.1021/cs3008297 | ACS Catal. 2013, 3, 1397−1405

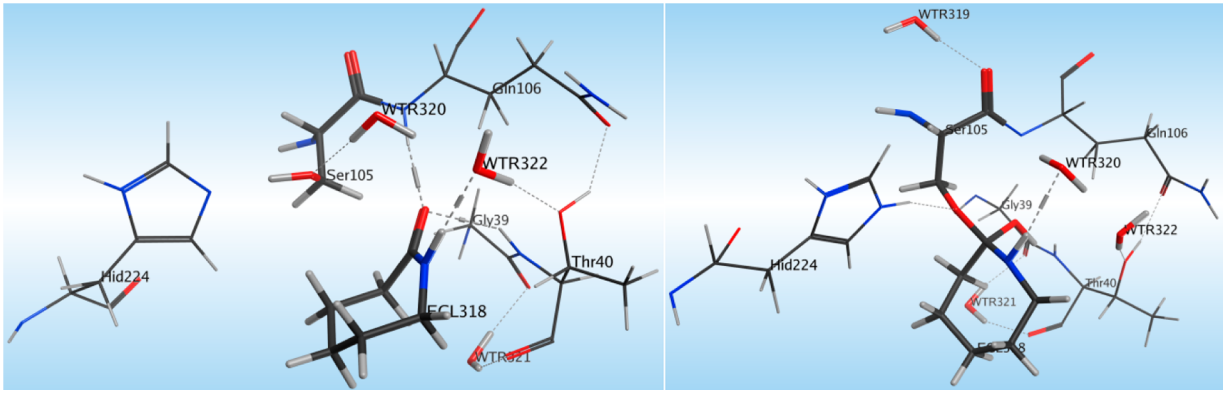

Figure 3. Reactant (**D**) (left) and Intermediate (**E**) (right) of the reaction sequence depicted in Scheme 3.

proton transfer from HN(Gln106) to the carbonyl oxygen of the lactam leaving a negative charge on the Glutamate nitrogen, N(Gln106), (Scheme 3, **E**). In the intermediate (**E**) the H-bond from the former carbonyl group of the lactam to N(Gln106) is reduced to 2.77 Å while still being 3.09 Å to N(Thr40) (Figure 3). Although, the proton transfer from the Glutamate nitrogen, N(Gln106), (Scheme 3, **E**) occurred spontaneously, this reaction step is very unusual. Therefore, in a consecutive calculation we have tried to move the migrating HN(Gln106) proton back to the glutamate nitrogen N-(Gln106) by using constraints. However, none of these attempts was successful but rather resulted in the displacement of the lactam from Ser105 and restoring of the reactant state (**D**).

To open the lactam ring another spring of 3.0 Å was applied to the breaking lactam C−N bond. During optimization of the resulting complex after removal of the constraint the distance of the breaking N−C bond increased to 3.17 Å and several proton transfers occurred. The proton from the carbonyl has shifted back to Gln106, a water proton has been transferred to the lactam nitrogen, and the HE2(His224) proton has moved to neutralize Wat320. (Scheme 3, structure (**F**) and Figure 4). In

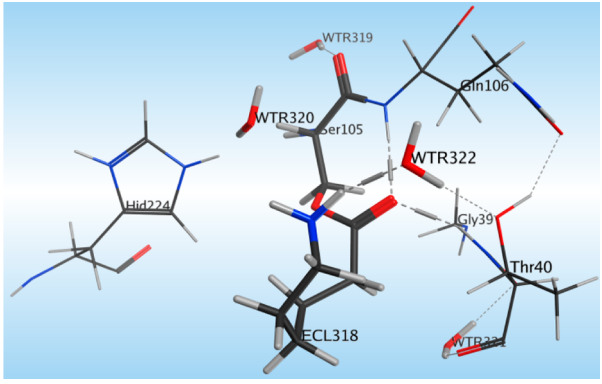

Figure 4. Acyl-enzyme complex (**F**) after ring-opening of the lactam.

this ring opened stable intermediate the lactam amino group is H-bonded to Wat322 (2.87 Å) and the carbonyl group is building up strong hydrogen bonds to NH(Gln106) (2.83 Å) and NH(Thr40) (2.83 Å).

Reversed Reaction, Ring Closure. To cross-check our findings we also calculated the reverse process, that is, the CALB catalyzed ring closure reaction of a Ser105 bound 6-aminocaproic-acid to form ε-caprolactam. Starting from the ring opened acyl-enzyme complex (Scheme 3, structure (**F**)) a spring of 1.4 Å was applied to the former C−N lactam bond. The resulting structure, however, did not match the tetrahedral intermediate of the forward reaction (Scheme 3, structure (**E**)) of the ring-opening mechanism but rather yields a new stable intermediate (Scheme 4, structure (**G**) and Figure 5), in which the former carbonyl oxygen of the lactam is negatively charged and ring closure already has occurred. This tetrahedral intermediate (**G**) resembles the one reached in the acylation reaction using caprolactone (see Scheme 2). Interestingly, we have not observed any proton transfer from the glutamate nitrogen N(Gln106) to the carbonyl oxygen. The negative charge on the lactam carbonyl was stabilized by strong hydrogen bonds to N(Gln106) and N(Thr40), both of 2.77 Å. In addition the carbonyl is weakly H-bonded to OW-(Wat322) 3.40 Å and OG(Thr40) 3.46 Å. The positive charge on the ring nitrogen is stabilized by Wat322 (N(lactam)−OW(Wat322) is 2.72 Å).

The reaction is terminated by transfer of the lactam proton from the amino group back to Wat320 thereby regenerating reactant state (**D**). Superposition of this structure with the starting complex (from the beginning of the ring-opening calculations) proved that the initial starting structures was almost identically regenerated with an RMSD as low as 0.04 Å between the two complex structures.

Reaction Energetics, ε-Caprolactone vs ε-Caprolactam. Experimental studies show that CALB does not catalyze the ring-opening polymerization of ε-caprolactam but does facilitate the ring closure.[34] However, ε-caprolactone can be enzymatically polymerized by CALB with high molecular weight and excellent yield. Therefore, a comparison of the reaction energetics should help to explain this difference.

The results of the transition state search and reaction barrier calculations are in excellent agreement with all experimental studies.[24−26] The free energy profile of the NEB (nudged elastic band)[35,36] optimized pathway was obtained by calculating the free energy difference between the consecutive NEB beads (calculation steps) in all cases.

Figure 6 shows that the rate limiting step of the acyl-enzyme (**C**) generation is the removal of the HG(Ser105) proton from OG(Ser105) (12 kcal/mol) in the process of the nucleophilic attack of the remaining anion on the lactone carbonyl. The reaction starts with the elongation of the HG(Ser105)−OG(Ser105) bond. At the transition state (TS1, bead 5) the proton is shared between OG(Ser105) and NE(His224). In the next step this transfer is almost completed, the OG(Ser105)−C(lactone carbonyl) bond starts to be generated in bead 7

dx.doi.org/10.1021/cs3008297 | ACS Catal. 2013, 3, 1397−1405

Scheme 4. CALB Catalyzed Ring Closure of Serine Bound 6-Aminocaproic Acid (F)

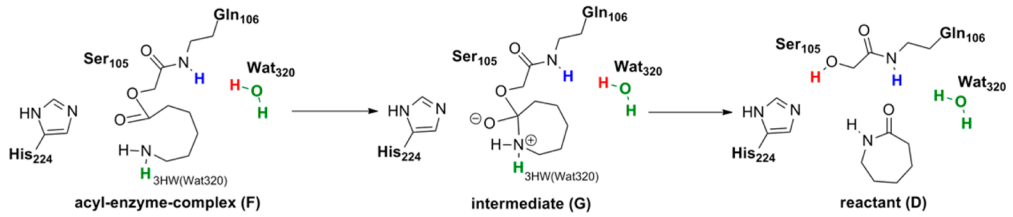

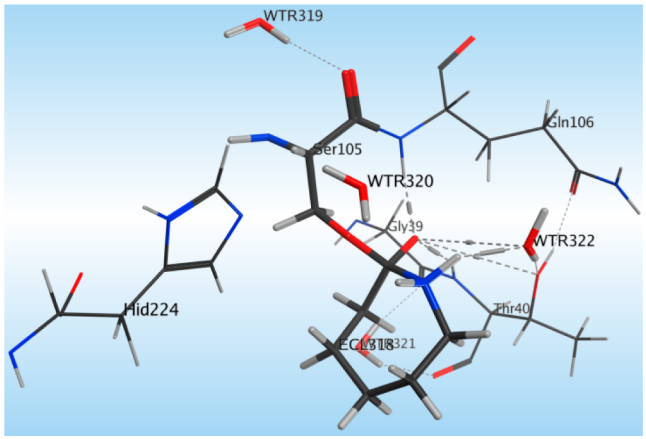

Figure 5. Tetrahedral intermediate (**G**) along the ring closure mechanism.

(TS2), and the reaction goes over a smaller barrier height (11 kcal/mol). Then the stable intermediate (**B**) is formed step by step in the consecutive beads.

The ring-opening procedure proceeds with even less hindrance (almost 2 kcal/mol) where in the transition state (TS3, bead 6) the migration proton HG(Ser105) is shared between the lactone oxygen and NE(His224). At this point the C−O distance is already 1.87 Å long, and the lactone ring begins to open. A significant change occurs at bead 7, where the lactone ring C−O bond entirely breaks and the proton transfer to the lactone ring oxygen almost completes. Afterward, the resulting acyl-enzyme complex is stepwise optimized to product (**C**). Our barrier height for the rate limiting step (the formation of the first tetrahedral intermediate, TI1) is also consistent with the findings of Hu et al.[28] (13.4 kcal/mol) who studied the ester hydrolysis in serine hydrolases using ab initio and DFT methods. However, they used a smaller system and propose that the generation of TI1 is a very shallow minimum on the potential energy surface.

As a next step, we performed a transition state search using the NEB method (nudged elastic band) and free energy calculations along the calculated pathways from reactant (**D**) via intermediate (**E**) to the acyl-enzyme complex (**F**) as well as the reverse reaction from (**F**) via intermediate (**G**) back to reactant (**D**).

Figure 7 shows the QM/MM energy profile for the two reaction steps involved in the forward reaction form (**D**) to (**F**). As a result we calculated the reaction barrier of the nucleophilic attack of Ser105 on the lactam carbonyl generating intermediate (**E**) to be as high as 27 kcal/mol (Figure 7, left) while the ring-opening reaction that leads to the acyl-enzyme complex (**F**) afforded a reaction barrier that is even slightly higher with 28 kcal/mol (Figure 7, right). It is rather unlikely that such a high reaction barrier can be overcome in an enzymatic reaction which suggests that the experimentally shown hindrance of the CALB catalyzed polyamide synthesis from caprolactam presumably does not proceed because of an energetically unlikely ring-opening step.

A detailed inspection of this reaction reveals that it starts slowly with an elongation of the HG(Ser105)−OG(Ser105) bond. Simultaneously, the lactam moves closer to Ser105 to be prepared for the nucleophilic attack. At the transitions state TS1 (Figure 7 left, bead 9) the HG(Ser105) proton is shared between Ser105 and His224 (HG(Ser105)−OG(Ser105) is 1.21 Å and HG(Ser105)−NE2(His224) is 1.41 Å. Figure 8 shows that in bead 10 the migrating proton moves closer to His224 where HG(Ser105)−OG(Ser105) increases to 1.39 Å

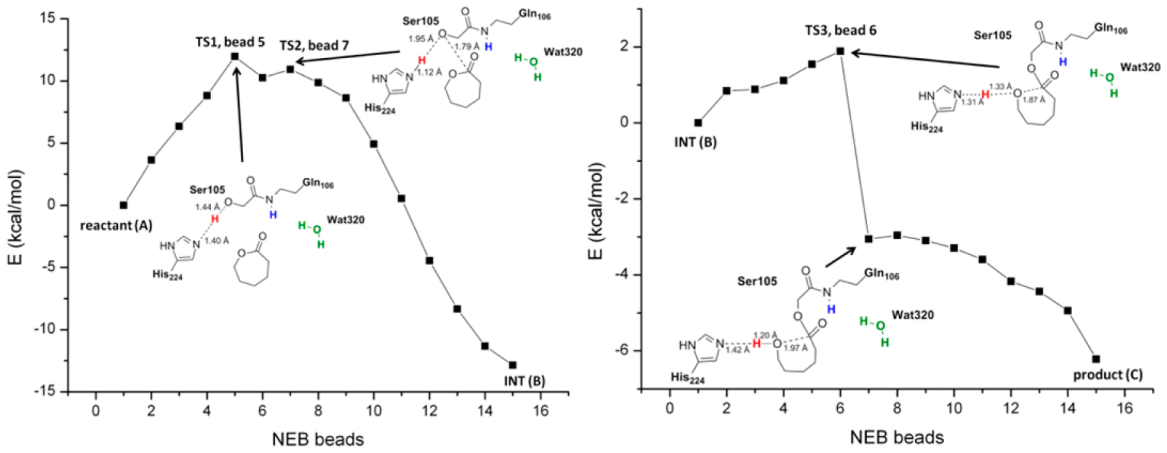

Figure 6. Reaction energies of acyl-enzyme generation along the CALB catalyzed ROP polymerization of ε-caprolactone. (Left) generation of intermediate (**B**), (right) ring-opening and acyl-enzyme formation (**C**) (see lac_rs-anb.xyz and lac_anb-ro.xyz in the Supporting Information).

dx.doi.org/10.1021/cs3008297 | ACS Catal. 2013, 3, 1397−1405

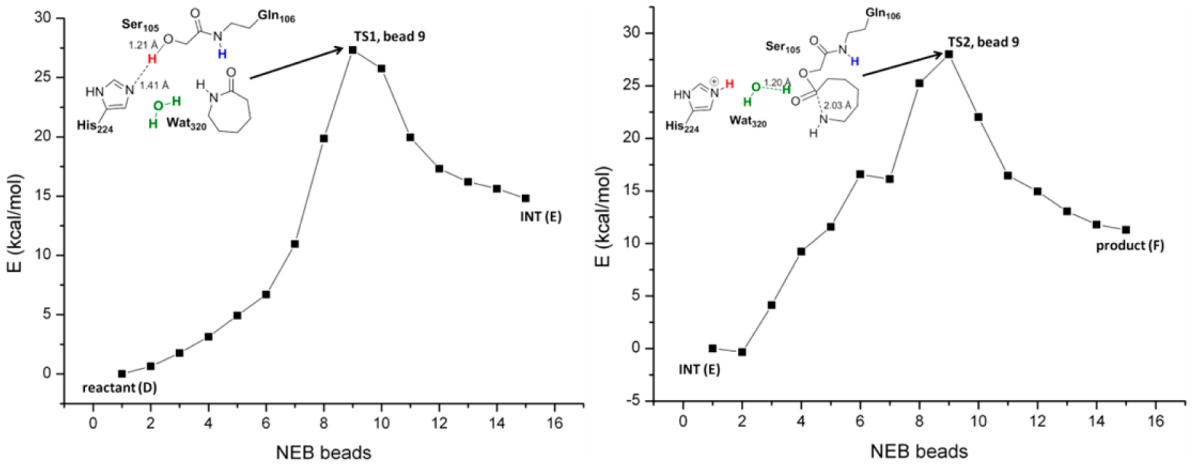

Figure 7. Reaction energies of acyl-enzyme generation along the CALB catalyzed ROP polymerization of ε-caprolactam. (Left) generation of intermediate (**E**), (right) ring-opening and acyl-enzyme formation (**F**). (see eCL_rs-anb.xyz and eCL_anb-ro.xyz in the Supporting Information).

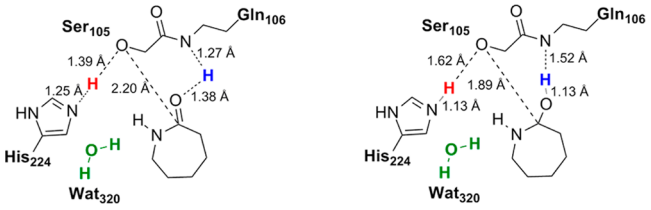

Figure 8. Bead 10 and bead 11 (see Figure 7, left) along the formation of the first tetrahedral intermediate for the ROP of ε-caprolactam.

and HG(Ser105)−NE2(His224) shortens to 1.25 Å and at bead 11 Gln106 transfers its HN(Gln106) proton to the lactam nitrogen (N(Gln106)−HN(Gln106) is 1.52 Å and HN-(Gln106−O(lactam) is 1.13 Å). It is remarkable that the proton transfer from Gln106 to the carbonyl oxygen proceeds in this reaction before the carbonyl-group is attacked by Ser105. At this point the lactam carbonyl is still 2.22 Å away from OG(Ser105). Subsequently, the nucleophilic attack starts generating the intermediate (**E**) which is optimized in the consecutive beads.

The acyl-enzyme formation is terminated by the extension of the lactam bond, the transfer of the proton from the carbonyl back to Gln106, and the reorientation of Wat320. This water molecule moves closer to Gln106 and the lactam to coordinate the proton transfer between them. At the transition state TS2 (Figure 7, right, bead 9) the lactam C−N bond is already completely broken, and the HW(Wat320)proton begins to transfer to the lactam nitrogen (HW(Wat320−OW(Wat320) 1.20 Å). This process is completed in the following bead, and the remaining OH^- of Wat320 accepts a proton from His224 to be neutralized.

To compare these results with the backward reaction from acyl-enzyme complex (**F**) via intermediate (**G**) to reactant state (**D**) we also calculated the path energies of the ring closure and found that this reaction has a considerably lower reaction barrier (14 kcal/mol) than the ring-opening (Figure 9). A ring closure reaction, therefore, is energetically easily achievable and should proceed in one step. When the reaction begins the N−HW(Wat320) bond of the lactam expands and the HW-(Wat320) proton starts to move toward Wat320.

At the highest point of the curve (TS, bead 8, see Figure 9) the OW(Wat320)−HW(Wat320) is 1.42 Å, the N−HW-(Wat320) bond is already completely broken (2.20 Å), the lactam ring starts to close, C−N is 1.86 Å, and OG(Ser105) begins to detach from the lactam carbonyl, OG(Ser105)−C(lactam) is 1.79 Å. In the next step (bead 9) the lactam ring is

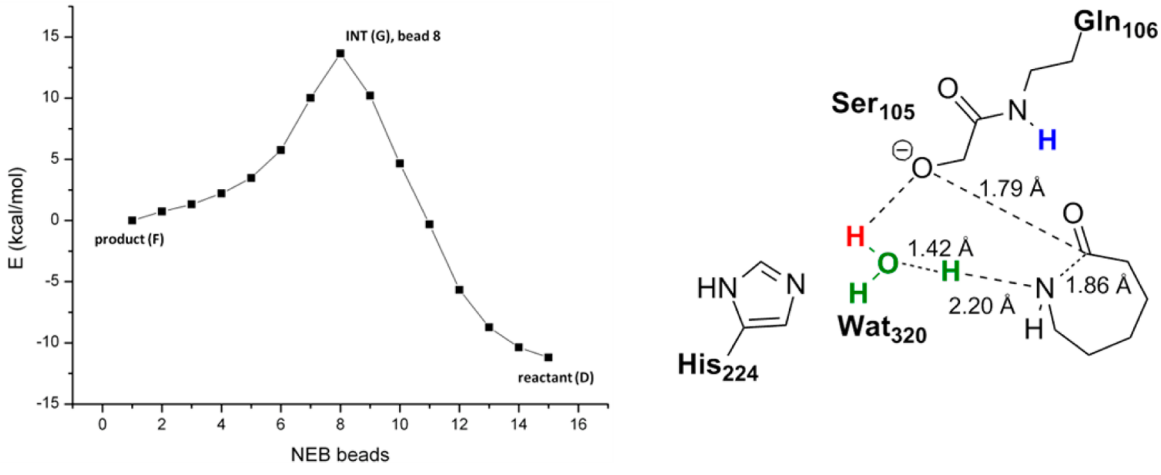

Figure 9. Reaction energy profile of the ring closure reaction starting from Ser105-bound 6-aminocaproic acid (left) and the structure of the corresponding transition state (TS) (right) (see eCL_rc.xyz in the Supporting Information).

dx.doi.org/10.1021/cs3008297 | ACS Catal. 2013, 3, 1397−1405

closed, and Wat320 is positively charged. Afterward (in bead 10), a proton from Wat320 migrates to Ser105 to neutralize the negative charge on OG(Ser105) and to generate the product state of the ring closing mechanism. In the following steps this state is optimized to an energy minimum structure. It is worthwhile to remark that His224 is not involved in this part of the reaction mechanism. However, we know that this residue is essential for the catalytic cycle to proceed.

COMPUTATIONAL METHODS

Structural Model. The crystallographic structure of *Candida Antractica* Lipase B (2.60 Å) complexed with a covalent bonded phosphonate inhibitor was used as starting structure for our calculations (PDB code 1LBS[37]). Hydrogen atoms were added to the heavy atoms. To use the original position of crystal water these coordinates were applied from the native enzyme (CALB) structure (PDB code 1TCA, 1TCB[38]). Since the overall charge of the enzyme was neutral the addition of counterions was not necessary, and the complex was solvated in an 80 Å cubic box of water (containing 11723 water molecules) centered on the active site. According to prior investigations of other groups[38,39] Asp134 was set protonated, and His224 was protonated on the ND side only. MD simulations followed by QM/MM optimization showed that the applied water positions were appropriate.

A. Water Molecules. All four water molecules applied from the crystal structure of the native enzyme were included into the QM region in all calculations.

B. Quantum Mechanical Region. A total of 110 atoms were treated quantum mechanically (QM region). The forces in the QM subsystem were calculated at the DFT/PBE0 level using Ahlrich's pVDZ basis set. The residues Ser105, Asp134, ECL318 (ε-caprolactam), and the 4 conserved water molecules (Wat319, Wat320, Wat321, Wat322) were added completely into the QM region and the fragments of Thr40, Trp104, Gln106, Gly107, Pro133, Tyr135, Gln157, and His224.

C. Mobile Region. The remaining protein atoms (4595 atoms) and the solvent molecules of the water box were included in the molecular mechanics region (MM region) and computationally treated by the AMBER99 force field.

MD and QM/MM Calculations. The bonds between the QM and MM subsystems were capped with H atoms.[40] In the first step of the calculation the entire solvent-enzyme−substrate structure was equilibrated by performing a series of molecular dynamics (MD) annealing runs for 100 ps at temperatures 50 K, 150 K, 200 K, 250 and 298.15 K with fixed positions of the atoms in the QM region. Afterward, the atomic positions in the MM region were fixed, and the atomic positions in the QM region were optimized at the PBE0 level; wave functions were expanded using the Ahlrich's pVDZ basis set. Then the resulting equilibration stage of the structure was optimized using a multiregion optimization algorithm as implemented in NWChem.[33] This method performs a sequence of alternating optimization cycles of the QM and MM regions. The effective charges were recalculated in each optimization cycle by fitting the electrostatic field outside the QM region to that produced by the full electron density representation. Several cycles of this optimization were carried out until convergence was obtained.

Spring Method. Starting from the reactant state a sequence of constrained optimizations were performed to study the ring closing and ring-opening mechansim. Harmonic restraints between the atoms of the breaking or newly generated bonds were imposed to drive the system over the transition states and reaction barriers to the intermediate and product states while at the same time allowing the MM system (initially equilibrated to the reactant structure) to adjust to the changes. When a reasonable estimate of the structure was obtained, the constraints were lifted, and the system was optimized using a sequence of optimizations and dynamical relaxation steps similarly to those discussed above.

NEB Calculations. To obtain an unbiased view of the reactive process, we have used the implementation of the NEB approach[35] within the NWChem QM/MM module. The NEB method optimizes the trial reaction pathway between two fixed points. In our simualtions we calculated 15−15 replicas connected by harmonic spring forces between reactant and intermediate and between intermediate product states. To ensure full relaxation of the protein environment, the first NEB optimization pass was followed by 20 ps of molecular dynamics equilibration at room temperature of the MM region for each of the beads along the pathway. After this equilibration, another round of NEB optimization was performed.

Free Energy Calculations. The free energy profile over the NEB optimized pathway was obtained by calculating free energy differences between the consecutive NEB beads. This approach is similar to the multilevel perturbation methodology, which has been used by Valiev et al.[41] for reactions in solutions.

Docking Calculations. Quick eXPlore (QXP)[42] starting from the X-ray structure taken from the Protein Database (PDB Code: 1LBS[37]), the model system was defined as a 15 Å cut around the catalytic pocket. The docking volume was defined by coloration of the so-called "guided atoms". The protonation of the residues was also calculated by QXP. For the docking procedure QXP uses the Monte Carlo method and employs a modified AMBER force field.[43] The docking run consists of several steps. The first step is sdock, which performs an initial placement of the desired ligand molecule. The first hit of this simulation is applied in the following full-Monte Carlo-Search (mcdock) step, in which QXP carries out an unrestrained conformational search. The best 1−4 hits were chosen for the subsequent local Monte Carlo-Search step (mcldock). In this second docking run the degrees of freedom are restricted (the ligand bonds can be turned by 20°−30° only). The best results were undertaken for multistep rescoring procedure[32] to reach the desired reactant state structures.

The ligands (ε-caprolactone and ε-caprolactam) were constructed using the Build panel and energy minimizer (MMFF94) of MOE2010.10.[44]

CONCLUSION

Although lactones can be polymerized enzymatically by CALB with high molecular weights the analogous enzymatic polymerization of a lactam has not yet been described. The only appreciable exception is the CALB catalyzed polymerization of β-lactam which resulted in an oligomer with only a maximum chain length of 18 monomer units and an average length of 8 units.[14] In this respect it is interesting to know that ω-amino acids of certain length can be cyclized to the corresponding lactams. Stavila and Loos[34] attempted the polymerization of 6-aminocaproic acid by CALB catalysis but instead ended up with the ring closing product, ε-caprolactam, in good yields. The formation of different other lactam rings from 4-aminobutanoic acid, 5-aminovaleric acid, and 8-aminooctanoic acid has also been reported in this publication.

In the present paper we analyzed this phenomenon using computational methods, such as docking approaches, molecular dynamic simulations, and QM/MM methods at DFT/B3LYP level of theory. In the procedure we follow our simulation of the CALB catalyzed β-lactam oligomerization in which we could show that the crucial point of the catalytic cycle is the generation of the first tetrahedral intermediate (TI1) from the attack of Ser105 at the lactam carbonyl.[12] Therefore, we have exemplarily used ε-caprolactone and ε-caprolactam to investigate the formation of the analogous intermediate, (B, E, and G, respectively).

For both substrates the reactions begins with a nucleophilic attack of OG(Ser105) on the substrate carbonyl and a simultaneous proton shift from Ser105 to His224. However, the ring-opening step proceeds in a different way for ε-caprolactone and ε-caprolactam reaction, respectively. In case of the lactone, the ring-opening takes place through the

dx.doi.org/10.1021/cs3008297 | ACS Catal. 2013, 3, 1397−1405

expected direct proton transfer from NE2(His224). No water is necessary to facilitate the proton shuttle because the lactone is positioned in an adequate place with correct orientation to easily allow the reaction. Because of the direct proton transfer this reaction proceeds via a very low reaction barrier of 12 kcal/mol.

In case of the lactam ring, however, our simulation suggests that, in contrast to the lactone substrate, the lactam is complexed in the active site in an orientation with a lactam nitrogen positioned away from His224 rather than toward the histidine as in case of the lactone oxygen. This is presumably induced by strong interaction with Gly39 and Thr40. As a consequence a direct proton transfer from His224 to the lactam is prevented but rather affords a water molecule (Wat320). In addition, in our calculation Gln106 delivers an amid-proton to the substrate to yield tetrahedral intermediate E without involvement of His224. Such a mechanism is only a little realistic and more importantly the calculated activation energy for this process is too high (27 kcal/mol) to be overcome in an enzymatic process. The fact that no other reaction pathway could be found in the computational calculation, suggests that an acylation of CALB Ser105 by ε-caprolactam is an energetically disfavored process, which is in contrast to the analogous reaction with ε-caprolactone.

This assumption is also supported by our calculation of the reverse process in which we find an energetically favored displacement of 6-aminocaproic acid from Ser105 by a water molecule and formation of ε-caprolactam. This result is also in good agreement with the experimental findings of Stavila and Loos.[34]

In conclusion, using a combined docking method and QM/MM simulations we found computational evidence of why the polymerization of ε-caprolactam is energetically hindered in comparison with the ring closure mechanism of 6-aminocaproic acid. A possible solution to overcome the difficulties of the CALB catalyzed ring-opening polymerization of ε-caprolactam could be a computational calculation along the lines of an in silico rational design to suggest exchange of one or more amino acids of CALB that finally might allow a mechanism of Ser105 acylation by ε-caprolactam as it is suggested for ε-caprolactone.

■ ASSOCIATED CONTENT

Supporting Information

Further details are given in chemical structure .xyz files. This material is available free of charge via the Internet at http://pubs.acs.org.

■ AUTHOR INFORMATION

Corresponding Author

*E-mail: elsaesse@mail.upb.de.

Author Contributions

The manuscript was written through contributions of all authors. All authors have given approval to the final version of the manuscript.

Notes

The authors declare no competing financial interest.

■ ACKNOWLEDGMENTS

B.E. was supported by a postdoc scholarship of the University of Paderborn. The calculations were carried out at the Paderborn Center for Parallel Computing (PC2) and at MSCF in the EMSL User Facility sponsored by the U.S. DOE.

■ ABBREVIATIONS

CALB Candida Antarctica Lipase B; QM/MM quantum mechanics molecule mechanics; DFT density functional theory; NEB nudged elastic bend

■ REFERENCES

(1) Elias, H. G. *Makromoleküle, Band 3*, 6. Auflage; Wiley-VCH Verlag: Weinheim, Germany, 2001.
(2) Zimmermann, J.; Kohan, M. I. *J. Polym. Sci., Part A* **2001**, *39*, 2565−2570.
(3) Kobayashi, S.; Uyama, H.; Kimura, S. *Chem. Rev.* **2001**, *101*, 3793−3818.
(4) Gross, R. A.; Kumar, A.; Kalra, B. *Chem. Rev.* **2001**, *101*, 2097−2124.
(5) Varma, I. K.; Albertsson, A.-C.; Rajkhowa, R.; Srivastava, R. K. *Prog. Polym. Sci.* **2005**, *30*, 949−981.
(6) Matsumura, S. *Adv. Polym. Sci.* **2006**, *194*, 95−132.
(7) Binns, F.; Harffey, P.; Roberts, S. M.; Taylor, A. *J. Polym. Sci., Part A: Polym. Chem.* **1998**, *36*, 2069−2079.
(8) Dong, H.; Cao, S. G.; Li, Z. Q.; Han, S. P.; You, D. L.; Shen, J. C. *J. Polym. Sci., Part A: Polym. Chem.* **1999**, *37*, 1265−1275.
(9) Uyama, H.; Kobayashi, S. In *Enzyme-Catalyzed Synthesis of Polymers*; Springer: New York, 2006; Vol. *194*, pp 133−158.
(10) Kumar, A.; Gross, A. *Biomacromolecules* **2000**, *1*, 133−138.
(11) Thurecht, K. J.; Heise, A.; deGeus, M.; Villarroya, S.; Zhou, J. X.; Wyatt, M. F.; Howdle, S. M. *Macromolecules* **2006**, *39*, 7967−7972.
(12) Baum, I.; Elsässer, B.; Schwab, L. W.; Loos, K.; Fels, G. *ACS Catal.* **2011**, *1*, 323−336.
(13) Cheng, H. N.; Gub, Q.-M. In *Green Polymer Chemistry: Biocatalysis and Biomaterials*; Cheng, H. N., Gross, R. A., Eds.; ACS Symposium Series1043; American Chemical Society: Washington, DC, 2010; Chapter 18, pp 255−263.
(14) Schwab, L. W.; Kroon, R.; Schouten, A. J.; Loos, K. *Macromol. Rapid Commun.* **2008**, *29*, 794−797.
(15) Gu, Q.-M.; Maslanka, W. W.; Cheng, H. N. In *Polymer Biocatalysis and Biomaterials II*; Cheng, H. N., Gross, R. A., Eds.; ACS Symposium Series 999; American Chemical Society: Washington, DC, 2008; Chapter 21, pp 309−319.
(16) Schwab, L. W.; Baum, I.; Fels, G.; Loos, K. In *Green Polymer Chemistry: Biocatalysis and Biomaterials*; Cheng, H. N., Gross, R. A., Eds.; ACS Symposium Series1043; American Chemical Society: Washington, DC, 2010; pp 265−278.
(17) Kobayashi, S. *Macromol. Rapid Commun.* **2009**, *30*, 237−266.
(18) Forro, E.; Fulop, F. *Org. Lett.* **2003**, *5*, 1209−1212.
(19) Li, X. G.; Lahitie, M.; Kanerva, L. T. *Tetrahedron: Asymmetry* **2008**, *19*, 1857−1861.
(20) Park, S.; Forro, E.; Grewal, H.; Fulop, F.; Kazlauskas, R. I. *Adv. Syn. Catal.* **2003**, *345*, 986−995.
(21) Tasnadi, G.; Forro, E.; Fülöp, F. *Tetrahedron: Asymmetry* **2007**, *18*, 2841−2844.
(22) Uyama, H.; Takeya, K.; Kobayashi, S. *Bull. Chem. Soc. Jpn.* **1995**, *68*, 56−61.
(23) Hollmann, F.; Grzebyk, P.; Heinrichs, V.; Doderer, K.; Thum, O. *J. Mol. Catal. B: Enzym.* **2009**, *57*, 257−261.
(24) Kobayashi, S. *Macromol. Symp.* **2006**, *240*, 178−185.
(25) Panova, A. A.; Kaplan, D. L. *Biotechnol. Bioeng.* **2003**, *84*, 103−113.
(26) van der Mee, L.; Helmich, F.; de Bruijn, R.; Vekemans, J. A. J. M.; Palmans, A. R. A.; Meijer, E. W. *Macromolecules* **2006**, *39*, 5021−5027.
(27) De Santis, L.; Carloni, P. *Proteins-Structure Function and Genetics* **1999**, *37*, 611−618.
(28) Hu, C. H.; Brinck, T.; Hult, K. *Int. J. Quantum Chem.* **1998**, *69*, 89−103.
(29) Syren, P. O.; Hendil-Forssell, P.; Aumailley, L.; Besenmatter, W.; Gounine, F.; Svendsen, A.; Martinelle, M.; Hult, K. *ChemBioChem* **2012**, *13*, 645−648.
(30) Mcmartin, C.; Bohacek, R. S. *Chem. Abstr.* **1995**, *210*, 3-Comp.

(31) Veld, M. A. J.; Fransson, L.; Palmans, A. R. A.; Meijer, E. W.; Hult, K. *ChemBioChem* **2009**, *10*, 1330−1334.
(32) Alisaraie, L.; Haller, L. A.; Fels, G. *J. Chem. Inf. Mod.* **2006**, *46*, 1174−1187.
(33) Valiev, M.; Bylaska, E. J.; Govind, N.; Kowalski, K.; Straatsma, T. P.; Van Dam, H. J. J.; Wang, D.; Nieplocha, J.; Apra, E.; Windus, T. L.; de Jong, W. A. *Comput. Phys. Commun.* **2010**, *181*, 1477−1489.
(34) Stavila, E.; Loos, K. *Tetrahedron Lett.* **2012**, *54*, 370−372.
(35) Henkelman, G.; Jonsson, H. *J. Chem. Phys.* **2000**, *113*, 9978−9985.
(36) Henkelman, G.; Uberuaga, B. P.; Jonsson, H. *J. Chem. Phys.* **2000**, *113*, 9901−9904.
(37) Uppenberg, J.; Ohrner, N.; Norin, M.; Hult, K.; Kleywegt, G. J.; Patkar, S.; Waagen, V.; Anthonsen, T.; Jones, T. A. *Biochemistry* **1995**, *34*, 16838−16851.
(38) Uppenberg, J.; Hansen, M. T.; Patkar, S.; Jones, T. A. *Structure* **1994**, *2*, 293−308.
(39) Garcia-Urdiales, E.; Rios-Lombardia, N.; Mangas-Sanchez, J.; Gotor-Fernandez, V.; Gotor, V. *ChemBioChem* **2009**, *10*, 1830−1838.
(40) Valiev, M.; Garrett, B. C.; Tsai, M. K.; Kowalski, K.; Kathmann, S. M.; Schenter, G. K.; Dupuis, M. *J. Chem. Phys.* **2007**, *127*, 51102.
(41) Valiev, M.; Yang, J.; Adams, J. A.; Taylor, S. S.; Weare, J. H. *J. Phys. Chem. B* **2007**, *111*, 13455−13464.
(42) McMartin, C.; Bohacek, R. S. *J Computer-Aided Mol. Des.* **1997**, *11*, 333−344.
(43) Cieplak, P.; Caldwell, J.; Kollman, P. *J. Comput. Chem.* **2001**, *22*, 1048−1057.
(44) http://www.chemcomp.com.